Dissipation of the insecticide profenofos in tropical agricultural soils (Berambadi catchment, South India): insight from compound-specific isotope analysis (CSIA)

J. Masbou, C. Grail, S. Payraudeau, Laurent Ruiz, M. Sekhar, J. Riotte, Gwenaël Imfeld

Journal of Hazardous Materials 488 (2025) 137428

Contents lists available at ScienceDirect

Journal of Hazardous Materials

journal homepage: www.elsevier.com/locate/jhazmat

Dissipation of the insecticide profenofos in tropical agricultural soils (Berambadi catchment, South India): Insight from compound-specific isotope analysis (CSIA)

J. Masbou [a], C. Grail [a,b,d], S. Payraudeau [a], L. Ruiz [b,c], M. Sekhar [c,d], J. Riotte [c,e], G. Imfeld [a,*]

[a] Institut Terre et Environnement de Strasbourg (ITES), University of Strasbourg/ENGEES, CNRS UMR 7063, France
[b] G-EAU, INRAE - AgroParisTech - Cirad - IRD - Montpellier SupAgro - Univ Montpellier, Montpellier, France
[c] Indo-French Cell for Water Sciences, ICWAR, IRD, Indian Institute of Science, Bangalore, India
[d] Civil Engineering Department, Indian Institute of Science, Bangalore, India
[e] Géosciences Environnement Toulouse, UPS, CNRS, IRD, CNES, Toulouse 31400, France

HIGHLIGHTS

- Rapid dissipation of profenofos in soil, with half-life of 1.1 ± 0.6 days.
- Development of carbon CSIA of profenofos with precision of ± 0.3 ‰ for $\delta^{13}C$ values.
- Photolysis and biodegradation in soil of profenofos caused carbon isotope fractionation.
- Profenofos biodegradation in soil reached 96 %, 3 days after a field application.
- Experimental data aligned with model, showing minimal (< 0.02 %) profenofos leaching.

GRAPHICAL ABSTRACT

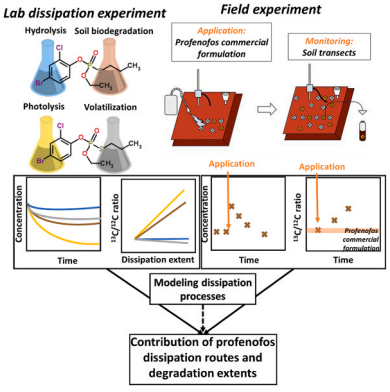

ARTICLE INFO

Keywords:
Pesticide
Soil
Organophosphates
Biodegradation
Photolysis
Stable isotopes
Modelling

ABSTRACT

Assessing the role of agricultural lands in pesticide contamination of water ecosystems is critical for water management agencies and policymakers when formulating effective mitigation strategies. Current approaches based on concentration measurements are often insufficient to evaluate the contribution of pesticide dissipation processes in complex agroecosystems. This study focuses on the dissipation of profenofos insecticide within plots subject to intensive agriculture in the Berambadi watershed (India). We examined profenofos dissipation kinetics and related carbon isotopic fractionation in laboratory volatilisation, hydrolysis, photolysis and soil biodegradation experiments, and in a field plot experiment. Process-specific isotope fractionation analyses revealed significant carbon isotope fractionation, with $\varepsilon_C = -2.0 \pm 0.8$ ‰ during UV photolysis, and $\varepsilon_C = -0.9 \pm 0.4$ ‰ during biodegradation of profenofos in the soil. Accordingly, the formation of 4-bromo-2-chlorophenol and another profenofos transformation product indicated the cleavage of O—P and C—Br bonds in soil experiments.

* Correspondence to: Institut Terre et Environnement de Strasbourg (ITES), 5, rue Descartes, Strasbourg cedex 67084, France.
E-mail address: gwenael.imfeld@cnrs.fr (G. Imfeld).

https://doi.org/10.1016/j.jhazmat.2025.137428
Received 10 December 2024; Received in revised form 23 January 2025; Accepted 27 January 2025
Available online 28 January 2025

By integrating dissipation kinetics, compound-specific isotope analysis (CSIA), transformation products analysis and modelling results, biodegradation was identified as the dominant dissipation process in the agricultural plot, accounting for > 90 % of profenofos dissipation. Model predictions were consistent with the observed dissipation kinetics and isotopic data, confirming the fast degradation ($T_{1/2}$ = 1.1 ± 0.6 day) and low (< 0.02 %) leaching potential of profenofos, which was not detected in the local groundwater monitored by passive samplers (POCIS). Overall, these results highlight the usefulness of profenofos CSIA to identify and unravel dissipation processes in tropical agroecosystems for improving contamination risk assessment.

1. Introduction

Organophosphate pesticides (OPs) are among the most widely commercialised pesticides and are commonly used in agriculture. Due to their high water solubility, OPs pose significant health risks and induce toxicity in non-target organisms including humans [1]. The persistence of OPs in agricultural soils, along with their transport to surface and groundwater, mainly depends on volatilisation and degradation processes [2]. OPs degrade rapidly upon exposure to sunlight and atmospheric conditions, as well as through microbial activity, depending on their bioavailability in soil [3]. Currently, assessing the occurrence, extent and pathways of OPs degradation in agricultural soils presents a major challenge [2,4], although it is essential to predict their persistence and the formation of transformation products (TPs). Conventional monitoring methods, which rely on concentration measurements, often fail to differentiate between true degradation and non-degradative processes such as volatilisation and sorption, which can significantly contribute to pesticide dissipation in soil [5].

Compound-specific isotope analysis (CSIA) of synthetic pesticides relies on the intrinsic isotopic composition at natural abundance of pesticide molecules and changes in the isotopic ratios of a given element (e.g., $^{13}C/^{12}C$) within the molecule [6,7]. CSIA enables tracking reaction-specific isotopic ratio changes within the persistent, non-degraded fraction of a pesticide in agricultural soil [5]. This approach may help assessing pesticide degradation processes involving molecular cleavage, especially in cases where mass balance reconciliation is difficult and where TPs undergoing further reactions are not detected [6]. Carbon CSIA has been applied to agricultural soil to investigate the transformation of pesticides such as chloroacetanilide [8-10] and triazine herbicides [11], pyrethroid and OP insecticides [12, 13], dimethomorph and procymidone fungicides [13,14]. Laboratory experiments on various OPs have demonstrated the potential of 2D CSIA [5], combining $\delta^{13}C$ and $\delta^{2}H$ measurements, to elucidate hydrolysis mechanisms [15,16]. While these studies established the proof-of-concept for soil CSIA of pesticides, they were often confined to artificially contaminated laboratory settings, such as soil microcosms or lysimeters, using pesticide concentrations far exceeding those typically found in the environment. In contrast, field studies remain scarce [8,14]. Notably, there is a lack of reference studies that investigate the contribution of degradative and non-degradative dissipation processes of widely used OPs in agricultural fields using CSIA.

Profenofos, O-(4-Bromo-2-chlorophenyl) O-ethyl S-propyl (S)-phosphorothioate, is a widely used OP insecticide that inhibits acetylcholinesterase activity, providing effective control of agricultural pests such as rice stem borer, leafroller, spider mite, and cotton bollworm [17,18]. Profenofos residues exhibit variable half-lives in soil, which may reflect their persistence in vegetables, soils, and groundwater, thereby posing significant risks to the quality and safety of agricultural products and drinking water [19-21]. Several approaches have been used to remove and degrade profenofos residues in the environment, including chemical oxidation, photocatalytic degradation, electron beam radiation, and nanomaterial sorption [22]. Biodegradation is recognized as an effective, cost-effective, and environmentally safe approach for remediating profenofos-contaminated environments [23]. However, the simultaneous occurrence of multiple dissipation processes in field settings complicates the monitoring of profenofos removal and the evaluation of the contributions of degradative and non-degradative dissipation processes. Consequently, comprehensive studies on the effective removal and degradation of profenofos in soil remain limited.

This study aimed to investigate the kinetics and processes of profenofos dissipation in a tropical agricultural soil using the CSIA approach. To achieve this, a CSIA method was developed to measure the carbon isotope composition of profenofos in agricultural soil. Reference laboratory experiments were conducted to examine the kinetics, pathways and carbon isotope fractionation associated with the major dissipation processes, including volatilisation, hydrolysis, photodegradation, and biodegradation. A field experiment was carried out in a beet root plot to quantify profenofos dissipation processes by integrating CSIA in a model calibrated using laboratory experiments data. The results demonstrate the ability of CSIA to distinguish between degradative and non-degradative processes, thereby improving the accuracy and reliability of contamination risk assessments for profenofos.

2. Material and methods

2.1. Chemicals

Extraction solvents, including dichloromethane (DCM), acetonitrile (ACN), ethyl acetate (EtOAc), pentane, methanol (MeOH), and ethanol (EtOH), were of HPLC grade purity (> 99.9 %) and were purchased from Sigma–Aldrich (St. Louis, MO, USA). Analytical standards, including S-metolachlor-d11, profenofos, and 4-bromo-2-chlorophenol, were of PESTANAL grades (purity > 98 %) and were also obtained from Sigma–Aldrich. The ROCKET 44 EC (Profenofos, 400 $g.L^{-1}$ + Cypermethrin 40 $g.L^{-1}$, PI Industries Ltd) was directly sourced from local farmers. Stock solutions at a concentration of 1 $g.L^{-1}$ were prepared in acetonitrile (ACN) and stored at – 20 °C. These stock solutions were subsequently used to prepare analytical calibrants and aqueous solutions for laboratory experiments. For the preparation of aqueous solutions, ACN from the stock spiking solution was removed by stirring the solution at room temperature for 30 min to facilitate evaporation.

2.2. Laboratory experiments

2.2.1. Profenofos volatilisation, hydrolysis and photolysis experiments

The volatilization, hydrolysis, and photolysis dissipation pathways of profenofos were investigated in laboratory experiments. All experiments were conducted at an environmentally relevant pH of 7, with additional tests—specifically hydrolysis and photolysis—performed at varying pH values to evaluate potential species dependencies. Profenofos does not exhibit pKa dissociation constants between 0.6 and 12, thus minimizing any pH-dependent species effects.

An experiment was conducted to investigate the profenofos volatilisation kinetics and associated carbon stable isotope fractionation. A pH 7 buffer solution (see Table S-1) was prepared with a profenofos concentration of 20 mg. L^{-1}. Aliquots of 1 mL of this solution were dispensed into 2 mL glass vials, which had been pre-burned at 450 °C for 2 h. The vials were covered with aluminum foils and left open in a fume hood at room temperature (20 ± 1 °C). Samples were collected in triplicate on days 0, 5, 15, 19, 23, and 35 using a sacrificial sampling approach. Additionally, control samples were collected in triplicate on days 0 and 35, which were subjected to the same conditions but kept in closed vials

with PTFE caps to prevent volatilisation.

Abiotic hydrolysis experiments were conducted in the dark within pre-burned (450 °C, 2 h) 60 mL amber glass vials. Three buffer solutions with pH values of 3, 7, and 9 were prepared (Table S-1 for buffer composition details) and spiked with 20 mg.L^{-1} of profenofos from a 1 g.L^{-1} stock solution. A 50 mL aliquot of the spiked buffer solution was carefully transferred into the amber glass vials, which were then sealed with screw caps, wrapped in aluminum foil, and incubated at 60 ± 1 °C. Samples were collected at regular intervals (t = 0, 1, 2.5, 4, 5.5, 7, 9, and 11 h) in triplicate using a sacrificial sampling approach. The pH values remained stable throughout the entire duration of the experiment at pH = 2.9 ± 0.1, pH = 6.8 ± 0.2, and pH = 9.2 ± 0.3.

Direct photolysis experiments were conducted at ambient temperature (20 ± 1 °C) using 254 nm ultraviolet (UV) light. The experimental setup included a light-tight enclosure (P/N 701 435, Jeulin) equipped with a low-pressure mercury lamp (LP Hg; P/N TUV G6T5, 6 W Phillips) emitting primarily at 254 nm, with secondary wavelengths contributing 22 % of the total output [24]. Borosilicate beakers (type 3.3, int. ⌀ = 37 mm) were filled with 50 mL of buffered solution (pH 3, 7, and 9, as for the hydrolysis experiment; Table S-1) and spiked with 20 mg.L^{-1} of profenofos. The beakers were placed inside the light-proof enclosure and irradiated from above. Samples (7 mL) were sequentially taken at t = 0, 3, 4.5, 6.5, 8.5 h. In parallel, dark controls covered with aluminium foil (except on the top), were placed in a light-proof fume hood and sampled at the same intervals.

A second direct photolysis experiment was conducted under simulated sunlight using a QSUN XE-1 test chamber (Q-LAB, Westlake, OH USA) equipped with a xenon arc lamp. The irradiation intensity was set to 0.68 W. m^{-2}.nm^{-1} at 340 nm to match peak solar irradiation, corresponding to approximately 1200 W. m^{-2} integrated over all wavelengths [25]. The temperature was maintained at 45 ± 5 °C. Profenofos photolysis was carried out in 500 mL pure quartz vials filled with 250 mL of pH 7 buffer spiked at 5 mg.L^{-1} of profenofos. Samples (7 mL) were collected at t = 16, 24, 43, 70, 137 and 209 h. Dark controls, covered with aluminium foil, were placed in the simulated sunlight chamber and sampled at the same times. All the vials were sealed with PTFE caps.

Blank control experiments, systematically conducted to assess potential cross-contaminations, were all falling below the limit of detection (LOD) and confirmed no cross-contamination. The incubation times were estimated based on a literature review [26].

2.2.2. Laboratory soil dissipation experiment

Topsoil samples (0–5 cm; n = 8) were collected in the field study plot in the Berambadi catchment on April 28th 2022, prior to the application of profenofos, for the soil degradation experiment. The physico-chemical characteristics of the soil, classified as red calcic Luvisol (FAO classification), are detailed in Table S-2. Background concentrations of profenofos in the collected soil sub-samples ranged from < 0.05 μg.kg^{-1} (i.e., < LOD) to 0.1 μg.kg^{-1}.

The soil degradation experiment was conducted at the Indo-French Cell for Water Sciences, Indian Institute of Science in Bangalore. Topsoil samples were pooled in a composite sample and then carted in six subsamples of 2 kg to conduct degradation experiments in triplicates. The experiments were set up in six clean, circular stainless-steel plates (30 cm internal diameter and 5 cm soil thickness), each covered with aluminium foils. Three heat-treated control experiments were conducted using soils that had undergone a triple heating cycle at 70 °C, each cycle lasting 72 h with 24 h intervals. This treatment was intended to limit microbial activity while minimizing changes to the soil physico-chemical properties [27]. Deionized water was added to achieve a volumetric water content equivalent to 20 % of the soil mass. The 3 biotic and 3 heat-treated soil experiments were spiked with a freshly prepared aqueous solution of the commercial formulation ROCKET 44 EC (2 mL.L^{-1}) to establish an initial concentration of 1 mg.kg^{-1} in soil on a wet weight basis, reflecting realistic environmental conditions following profenofos application.

The biotic and heat-treated experiments were incubated in parallel at 25 ± 1 °C (min = 22.5 °C, max = 27.5°C). Water loss during the experiment remained < 7 % by the end of the study. Soil aliquots (15 g) from the biotic and heat-treated experiments were collected on days 1, 5, 20, and 40, placed in clean glass vials, immediately frozen, and stored at – 20 °C until extraction and analysis.

2.3. Field experiments

2.3.1. Study area

The Berambadi experimental watershed (11°43'00"–11°48'00" N, 76°31'00"–76°40'00" E, 84 km^2) is located in Karnataka, southwestern India. It is part of the South Gundal basin (816 km^2), which belongs to the Kabini Critical Zone Observatory ([28]; SNO M-tropics, https://mtropics.obs-mip.fr/) (Fig. 1). Biophysical variables have been monitored since 2010 through the Environmental Research Observatory M-TROPICS [29], part of the OZCAR research infrastructure [30]. The study plot consisted of red sandy clay loam Luvisol, comprising 60 % sand, 15 % silt, and 25 % clay, with a pH range of 7.1–7.9 (Table S-2). Detailed information on the climatic, pedological, and hydrogeological characteristics of the study plot is provided in the SI.

2.3.2. Characteristics of the plot soil, profenofos application, and soil sampling

Topsoil samples (0–10 cm depth) were collected across the experimental plot (10 ×10 m) within the Berambadi watershed (Fig. 1). Composite soil samples (1 kg each) consisted of pooled topsoil subsamples systematically taken at 2 m intervals along three parallel transects within the plot. The sampling campaign began on May 23rd, 2022, one day before the profenofos application (denoted as t = – 1 day). The day – 1 composite sample was used to assess background profenofos concentration in the plot, determine extraction recoveries of profenofos from the soil, and evaluate potential carbon stable isotope fractionation associated with the soil extraction procedure (Table S-3).

On this plot, the local farmer applied profenofos to the bare soil just after beetroot sowing on 24th May 2022. The application was conducted within a single day in three successive passes, each separated by a 2 h interval. The commercial formulation, ROCKET 44 EC, was diluted with water at a ratio of 1:1000 (v/v) and applied at a rate of 0.57 L.m^{-2}. This corresponded to a profenofos dose of 2.4 kg.ha^{-1} or 243 mg.m^{-2}, which is five times the recommended application rate. Subsequent samples were collected on days 0 (3 h after the profenofos application), 1, 3, 7, 10, 15, 22, and day 34 (June 27th, 2022).

The agricultural practices encompass ploughing and the cultivation of one to three successive crops annually. These crops typically include rainfed crops and short-cycle irrigated crops, such as onions, beetroot and potatoes [31].

2.3.3. POCIS preparation and deployment

In-house Polar Organic Chemical Integrative Sampler (POCIS) devices were prepared as previously described [32] to evaluate the occurrence of pesticides in groundwater. Briefly, 250 mg of HyperSep™ Retain (Thermo Scientific) sorbent, equivalent to Oasis HLB sorbent (Waters), was used. The sorbent was sandwiched between two microporous polyethersulfone (PES) membranes (0.1 μm pore size, 90 mm, outside diameter, Pall Corporation) and secured tightly with two stainless steel rings (90 mm, outside diameter) and three screws. POCIS devices were deployed in triplicate for 28 days, from April 20th to May 24th, 2022, in six borewells of the Berambadi catchment at depths ranging from 30 to 75 m depending on the local groundwater table depth (Fig. 1). Due to the unavailability of on-site monitoring instruments, groundwater characteristics such as pH, depth, and other parameters could not be recorded during this study. Consequently, our analysis primarily focused on location-based observations.

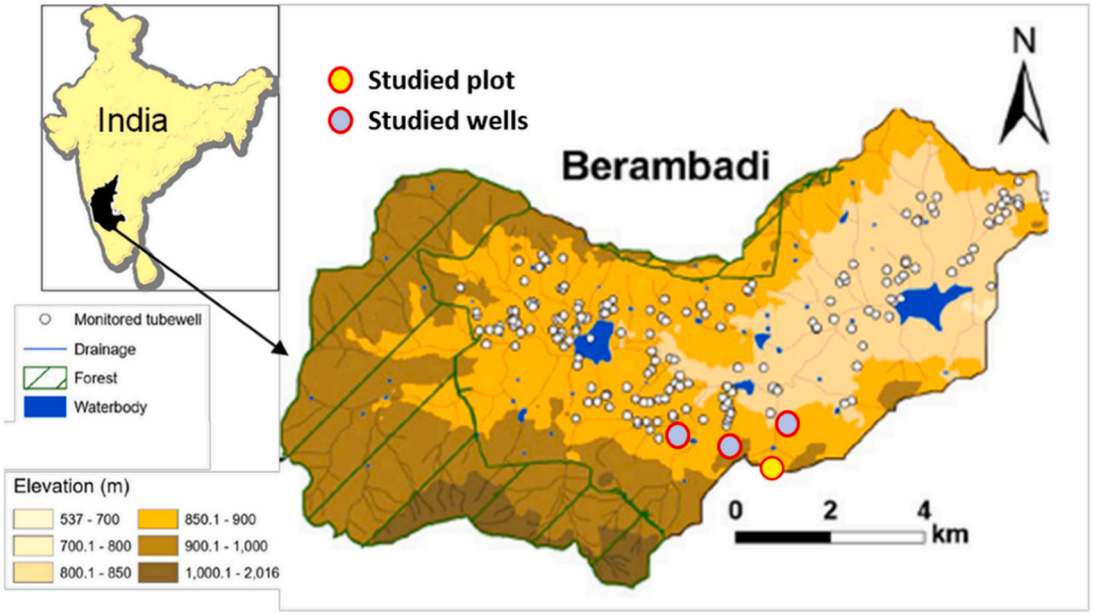

Fig. 1. The Berambadi watershed (Karnataka, India) with location of the experimental plot (10 ×10 m) and the studied groundwater wells.

2.4. Profenofos extraction and analytical methods

2.4.1. Profenofos extraction from water, soil and POCIS

Profenofos was extracted from water using a liquid-liquid extraction (LLE) method. Aqueous solutions ranging from 1 mL (volatilisation experiment) to 10 mL (photolysis experiment) were extracted with ethyl acetate (EtOAc) in 15 mL Falcon centrifuge tubes. The LLE procedure involves adding 3 mL of EtOAc, vortexing for 30 s, and centrifugation at 4000 rpm (2473 RCF) for at least 5 min or until phase separation. The EtOAc supernatant phase was carefully transferred to an amber glass vial, and the extraction procedure was repeated twice. The extracts were then evaporated to dryness under a gentle stream of nitrogen (grade 4.5) and reconstituted in 0.5 mL of ACN. A test to assess potential loss of profenofos during evaporation revealed no significant reduction in profenofos levels. Recovery rates are provided in Table S-3 and S-4.

Profenofos was extracted from soil samples using a previously described modified ultrasonic-assisted extraction protocol [33], with the modification that 5–10 g of soils were placed in an amber glass centrifuge tube prior to the addition of 1 mL of EtOAc per gram of sample.

The POCIS extraction procedure was adapted from [34]. Each POCIS was carefully opened, and the sorbent was transferred into an empty solid-phase extraction (SPE) cartridge, which was sealed on both sides with HDPE frits (AFFINISEP or Thermo Scientific). The samples were then processed using a SPE method [33,34]. Cartridges were dried under a gentle stream of nitrogen for 20 min, and pesticides were eluted (5 mL. min^{-1}) using successively 5 mL of EtOAc and 5 mL ACN. The extracts were evaporated to dryness under a gentle stream of nitrogen and reconstituted in 0.5 mL of ACN.

2.4.2. Profenofos quantification

Profenofos and its transformation product, 4-bromo-2-chlorophenol, were quantified with a gas chromatograph (GC, Trace 1300, 172 Thermo Fisher Scientific) coupled with a mass spectrometer (MS, ISQ™, Thermo Fisher 173 Scientific) [35]. Chromatographic separation was achieved using a TG –5MS column (30 m × 0.25 mm ID, 0.25 μ film thicknesses). The parameters for the GC and MS are provided in Table S-5 and S-6. An internal standard of S-metolachlor-d11 was prepared at 300 $\mu g.L^{-1}$ in ACN and injected with each sample to account for analytical bias. The detection of profenofos and quantification limits are provided in the Table S-3 and S-4.

2.4.3. Carbon CSIA of profenofos

Carbon stable isotope signatures of profenofos were measured using a GC-C-IRMS system, consisting of a TRACE™ Ultra Gas Chromatograph (ThermoFisher Scientific) coupled via a GC IsoLink/Conflow IV interface to an isotope ratio mass spectrometer (Delta V Plus, ThermoFisher Scientific). Chromatographic separation was performed on a TG-5MS column (60 m × 0.25 mm ID, 0.25 μm film thickness). Samples were injected in split/splitless modes depending on pesticide concentration, with an injection volume of 2 μL and injector temperature of 250 °C. A laboratory standard mix of benzene, toluene, ethylbenzene, and xylene (BTEX) was injected at the beginning of each session to verify the CO_2 conversion and overall analytical performance of the instrument. The stable isotope compositions of pesticide standards were calibrated relative to Vienna Pee Dee Belemnite (VPDB) scale with EA–IRMS (Flash EA IsoLink™ CN IRMS, Thermo Fisher Scientific) with a two-point calibration procedure with international reference materials AIEA600, USGS40, and USGS41. All isotopic measurements were reported in δ notation [36] relative to an international isotopic scale (Vienna Pee Dee Belemnite):

$$\delta^{13}C = \left[\frac{\left(\frac{^{13}C}{^{12}C}\right)_{sample}}{\left(\frac{^{13}C}{^{12}C}\right)_{VPDB}} - 1 \right] \times 1000 \quad (1)$$

EA-IRMS measurements for profenofos analytical standard yielded $\delta^{13}C = -22.6 \pm 0.2$ ‰ (n = 3). To ensure measurement accuracy, standards with isotopic compositions characterized by EA-IRMS were injected every six samples. The long-term reproducibility of profenofos GC-IRMS measurements was $\delta^{13}C = -23.1 \pm 0.5$ ‰ (n = 23) across all analytical sessions. Samples were measured three times, and the $\delta^{13}C$ values were reported as the arithmetic mean, accompanied by the standard deviation (SD) calculated from the replicate measurements.

Isotope fractionation values (ε_C) relating the change in $\delta^{13}C$ to the extent of degradation, were derived from the logarithmic form of the Rayleigh equation, without forcing the regression through the origin [37]:

$$\ln\left(\frac{\delta^{13}C_t + 1000}{\delta^{13}C_0 + 1000}\right) = \frac{\varepsilon_C}{1000} \ln\left(\frac{c_t}{c_0}\right) \quad (2)$$

where $\delta^{13}C_0$ and $\delta^{13}C_t$ represent the carbon isotope ratios for profenofos (expressed in ‰) at time 0 and t of degradation, respectively, and c_t/c_0 is the fraction of remaining profenofos at time t.

The isotope fractionation values (ε_C), obtained from the microcosm degradation experiments, were used in a modified form of the Rayleigh equation (Eq. 3) to quantify the fractional amount of profenofos degradation in the field, *F*, as a percentage of the initially present profenofos mass:

$$F = (1-f)\times 100 = \left(1 - \left[\frac{\delta^{13}C_t + \Delta(^{13}C_t) + 1000}{\delta^{13}C_0 + 1000}\right]^{\frac{1000}{\varepsilon_C}}\right)\times 100 \quad (3)$$

where *f* is the fraction of remaining profenofos in the agricultural soil.

2.5. Profenofos mass balance modelling

A parsimonious model [38] was adapted to estimate the components of the profenofos mass balance in the topsoil layer (0–10 cm) of the beetroot plot, including degradation, volatilisation, leaching and profenofos residual mass in the topsoil. Given the flat topography of the plot, daily rainfall was assumed to fully infiltrate the topsoil, contributing to the water mass balance in this layer (Eq. 4):

$$\frac{\Delta\theta}{\Delta t} = R - ET_0 - P \quad (4)$$

where the change in soil water content over time ($\Delta\theta/\Delta t$), rainfall (R), actual evaporation (ET_0) from bare soil, and percolation (P) were expressed in mm H_2O d^{-1}. Hydrological processes, such as percolation to deeper soil layers and evaporation, were calculated using methods from [39,40], respectively. Detailed equations are provided in Payraudeau et al. [38].

Daily climatic data, including rainfall and ET_0, were retrieved from the Berambadi flux tower station (Lat. 11.76°N; Lon. 76.59 °E, 2.6 km north-west from the plot). Soil properties were obtained from previous studies (Table S-2). The rate of change of profenofos mass ($\frac{\Delta M_{Profenofos}}{\Delta t}$) in the topsoil layer (mg.ha^{-1}.d^{-1}) was then given by:

$$\frac{\Delta M_{Profenofos}}{\Delta t} = A - V - LCH - DEG - PHO \quad (5)$$

where the profenofos mass applied (A), volatilisation (V), leaching to deeper soil layer (LCH), biodegradation (DEG), photolysis (PHO) are expressed in mg.ha^{-1}. Based on laboratory-scale volatilization closed control experiment at pH 7 and 20 °C, where no significant degradation was observed (Table 1), abiotic hydrolysis was deemed negligible under environmental conditions and was therefore excluded from the modelling approach. Detailed equations describing the dissipation processes are provided in the SI and in Payraudeau et al. [38].

2.6. Data analysis and statistics

Rate constants (*k*) and half-life ($T_{1/2}$) were determined using a Single First-Order Rate Model (SFO) from plots of ln (C/C_0) *versus* time. Slope significances and uncertainties were analysed using the Real Statistics Resource Pack for Microsoft Excel® available at http://www.real-statistics.com. In particular, the slope statistics comprised the calculation of standard errors for the slopes using the least squares method, and significance testing of the slopes using two-tailed p-values based on Student's t-distribution. All data were presented as mean ± SD unless otherwise specified.

Table 1
Profenofos dissipation kinetics ($T_{1/2}$) and isotope fractionation (ε_C) parameters derived from laboratory experiments (n.s = non-significant).

Matrix	Experiment	Conditions	$T_{1/2}$ ± 95 % CI (h or d)	ε_C (‰)
Water	Photolysis	pH 3, 254 nm, 20 °C, open	3.0 ± 1.0 h	− 1.9 ± 1.0
		pH 3, dark, 20 °C, open	n.s	n.s
		pH 7, 254 nm, 20 °C, open	3.5 ± 1.2 h	− 2.0 ± 0.8
		pH 7, dark, 20 °C, open	n.s	n.s
		pH 7, Xe light, 45 °C, closed	10.5 ± 2.9 d	n.d
		pH 7, dark, 45 °C, closed	n.s	n.s
		pH 9, 254 nm, 20 °C, open	2.8 ± 0.9 h	− 1.9 ± 0.8
		pH 9, dark, 20 °C, open	n.s	n.s
	Hydrolysis	pH 3, dark, 60 °C, closed	n.s	n.s
		pH 7, dark, 60 °C, closed	13.9 ± 0.9 h	n.s
		pH 9, dark, 60 °C, closed	1.8 ± 0.4 h	n.s
	Volatilisation	pH 7, dark, 20 °C, open	6.3 ± 3.0 d	n.s
		pH 7, dark, 20 °C, closed	n.s	n.s
Soil	Soil dissipation	Biotic, 25 °C, open	1.4 ± 0.6 d	− 0.9 ± 0.4
		Heat-treated, 25 °C, open	1.1 ± 0.2 d	n.s

3. Results and discussion

3.1. Developments and validation of profenofos CSIA from water and soil samples

The analytical method developed for profenofos CSIA allowed precise and accurate determination of $\delta^{13}C$ values in water and soil samples. The GC-C-IRMS response showed a linear increase in peak intensities with concentration, reaching a plateau in carbon isotope composition (Fig. 2). Injection with less than 5 ng of C on-column resulted in inconsistent $\delta^{13}C$ values, with reduced precision (> 2.5 ‰), reproducibility (SD = 1.0 ‰), and accuracy ($\Delta(^{13}C)_{EA\text{-}GC}$ > 2 ‰). Optimal performance was achieved with injections between 8 and 42 ng C, corresponding to profenofos concentrations of 11–56 mg.L^{-1}. Within this range, $\delta^{13}C$ values obtained using GC-IRMS (− 22.9 ± 0.3 ‰;

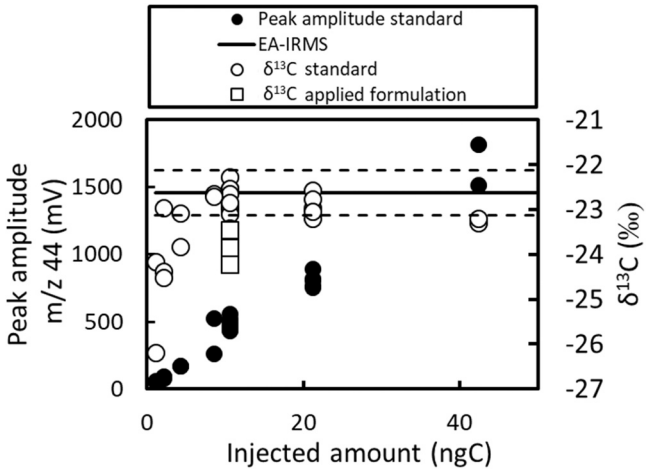

Fig. 2. Peak amplitude and carbon isotope composition ($\delta^{13}C$) as a function of the injected amount of profenofos. The commercial profenofos formulation (ROCKET 44) is represented by squares.

n = 22) did not significantly differ from those obtained with EA-IRMS (− 22.6 ± 0.2 ‰; n = 3). The total uncertainty of carbon isotopic measurements, including precision, accuracy, and reproducibility, was ± 0.3 ‰ (n = 3).

The extraction procedures for profenofos from water or soil samples had minimal impact on $\delta^{13}C$ values, with deviations ($\Delta\delta^{13}C$) of less than 0.7 ‰ for water extractions and less than 1 ‰ for soil extractions (Table S-3). The primary isotope source, the commercial formulation ROCKET 44, had a slightly different $\delta^{13}C$ value (− 23.8 ± 0.3 ‰; n = 6) compared to analytical standards, consistent with previous observations for other pesticides [41].

Overall, the validation assay results confirmed the suitability of the profenofos CSIA method for the monitoring dissipation processes in both laboratory and field experiments.

3.2. Kinetics of profenofos dissipation in laboratory experiments

The primary abiotic dissipation processes of profenofos in aqueous environments, including volatilisation, hydrolysis, and photolysis, were systematically quantified through dedicated laboratory experiments. Profenofos dissipation processes were characterized by varying half-lives ($T_{1/2}$) and carbon isotopic fractionation (ε_C) (Table 1).

3.2.1. Volatilisation

With a Henry's law constant of 6.2×10^2 mol.m^{-3}.Pa^{-1} [42], profenofos is considered as moderately volatile. However, laboratory experiments conducted at 20 °C showed rapid profenofos volatilisation from water, with half-life of 6.3 ± 3 d, suggesting volatilisation as a major dissipation route.

3.2.2. Hydrolysis

Volatilization control experiments conducted in sealed vials confirmed that abiotic hydrolysis was not a significant process at pH = 7 and T = 20 °C, over the 35 days of experiment. Since hydrolysis may depend on the prevailing pH conditions in the environment, further investigations were conducted to assess the effect of pH and temperature on profenofos hydrolysis. Raising the temperature to 60 °C led to substantial and rapid hydrolysis at pH = 7 ($T_{1/2}$ = 13.9 ± 0.9 h) in sealed vials. Such temperature conditions significantly accelerated the hydrolysis at pH = 9 with a $T_{1/2}$ = 1.8 ± 0.4 h, resulting in over 96 % of profenofos degradation within the 9 h incubation period. In contrast, at pH 3, profenofos dissipation was negligible (< 5 %) within the same period. This pH dependence aligns with previous studies, which showed increasing profenofos hydrolysis from pH 5–9 in water [43].

3.2.3. Photolysis

Photolysis experiments showed rapid dissipation of profenofos under UV light (254 nm) at 20 °C, with $T_{1/2}$ ranging from 2.8 to 3.5 h across pH values from 3 to 9. In contrast, under simulated sunlight (Xe lamp) at pH 7 and T° = 45 °C, less than 50 % of degradation was observed after 10 days of irradiation. This indicates that profenofos is not highly sensitive to photolysis under these conditions. The sensitivity of profenofos to UV photolysis at environmental pH was previously predicted by its relatively high molar extinction coefficient (ε = 460 M^{-1}.cm^{-1} at 254 nm) [44]. Leveraging this property, several studies have demonstrated the potential of UV-based solutions for remediating profenofos in drinking water [45].

3.2.4. Soil dissipation

Dissipation of profenofos in both biotic and heat-treated laboratory soil experiments was rapid, with $T_{1/2}$ = 1.4 ± 0.6 d and 1.1 ± 0.2 d respectively (Table 1), suggesting abiotic dissipation of profenofos under both soil conditions. With a soil pH range of 7.1–7.9 (Table S-2), abiotic hydrolysis can be excluded as a major pathway for the dissipation of profenofos. Nonetheless, mineral surfaces have been hypothesised to significantly accelerate hydrolysis kinetics ($T_{1/2}$ < 10 d) for some OPs and carbamate pesticides, which otherwise exhibit slow hydrolysis rates in aqueous solutions ($T_{1/2}$ > 1 y) [46]. However, the soil dissipation kinetics of profenofos were found to be in the same order of magnitude as those measured in the water volatilisation experiment ($T_{1/2}$ = 6.3 ± 3.0 days at 20 °C), confirming that volatilisation might be a dominant process driving profenofos dissipation in soil. In a previous study, volatilisation was shown to dominate dissipation in a 3 days experiment comparing heat-treated and biotic (inoculated with profenofos microbial degraders) soils, resulting in 88 % and 98 % of profenofos dissipation, respectively [47]. In our study, profenofos dissipation rates in both biotic and heat-treated soil experiments were an order of magnitude faster compared than those previously reported ($T_{1/2}$ = 7–15 d) in similar soil experiments [48]. However, the specific contribution of individual dissipation processes could not be clearly identified.

In addition to volatilisation, biodegradation may substantially contribute to profenofos dissipation in the biotic soil experiment. Notably, several microorganisms, including *Pseudomonas putida*, *Pseudomonas plecoglossicida*, *Pseudomonas aeruginosa,* have been enriched from contaminated soils and shown the ability to degrade profenofos [43,49].

Altogether, laboratory soil experiments showed that the rapid dissipation of profenofos was driven by both degradative and non-degradative processes. Further investigation of transformation products and the carbon isotope composition of profenofos could yield critical insights to disentangle and quantify these dissipation processes.

3.3. Potential of CSIA to assess profenofos transformation pathways in agricultural soil

For each profenofos transformation pathway, inferred from the detection of transformation products (Fig. 3), the corresponding bond cleavage and the expected kinetic isotope effect (KIE), calculated based on the Streitwieser Limit, were provided to interpret the observed carbon isotope fractionation (ε_C) during biotic and abiotic degradation processes.

3.3.1. Volatilisation

A $\Delta\delta^{13}C$ < 0.5 ‰ observed after 97 % dissipation of profenofos indicated that volatilisation from water does not cause significant isotope fractionation. This results aligns with the low isotope fractionations (ε_C < 0.38 ‰) reported in a previous study on NAPL compounds [54].

3.3.2. Hydrolysis

No significant carbon isotope fractionation was observed during profenofos hydrolysis, with $\Delta\delta^{13}C_{(end\ -\ initial)}$ < 0.7 ‰ across all experiments. This contrasts with previous studies on pesticide hydrolysis, which reported systematic carbon isotope fractionation (ε_C ranging − 2.1 to − 6.1 ‰) during both acidic and alkaline abiotic hydrolysis of triazine and chloroacetanilide pesticides [35,55]. However, it is consistent with ε_C values of − 0.2 ± 0.1 ‰ and − 1.0 ± 0.1 ‰ observed for the hydrolysis of the OPs dichlorvos and diethoate, respectively [56]. Profenofos hydrolysis primarily involves an O—P bond cleavage (pathway 1), producing 4-bromo-2-chlorophenol (BCP). The absence or low carbon isotope fractionation is consistent with a secondary isotope effect. Similar results were reported for abiotic hydrolysis of dichlorvos, where a O—P bond cleavage also resulted in ε_C = − 0.2 ± 0.1 ‰ [56]. Notably, the occurrence of BCP decreased from pH 9 to pH 3, where other TPs arising from C—O and C—S bond cleavages were detected. This pathway shift was also reflected by isotope data, with a more pronounced change in carbon isotope ratios ($\Delta\delta^{13}C_{(end\ -\ initial)}$ = +1.3 ‰) at the end of the hydrolysis at pH 3. These results are consistent, albeit with lower magnitudes, with the abiotic hydrolysis of parathion OP, where ε_C ranged from − 6.9 ± 0.8 ‰ at pH 2 to − 3.5 ± 0.4 ‰ at pH 9, and to the absence of isotope fractionation at pH 12 [16].

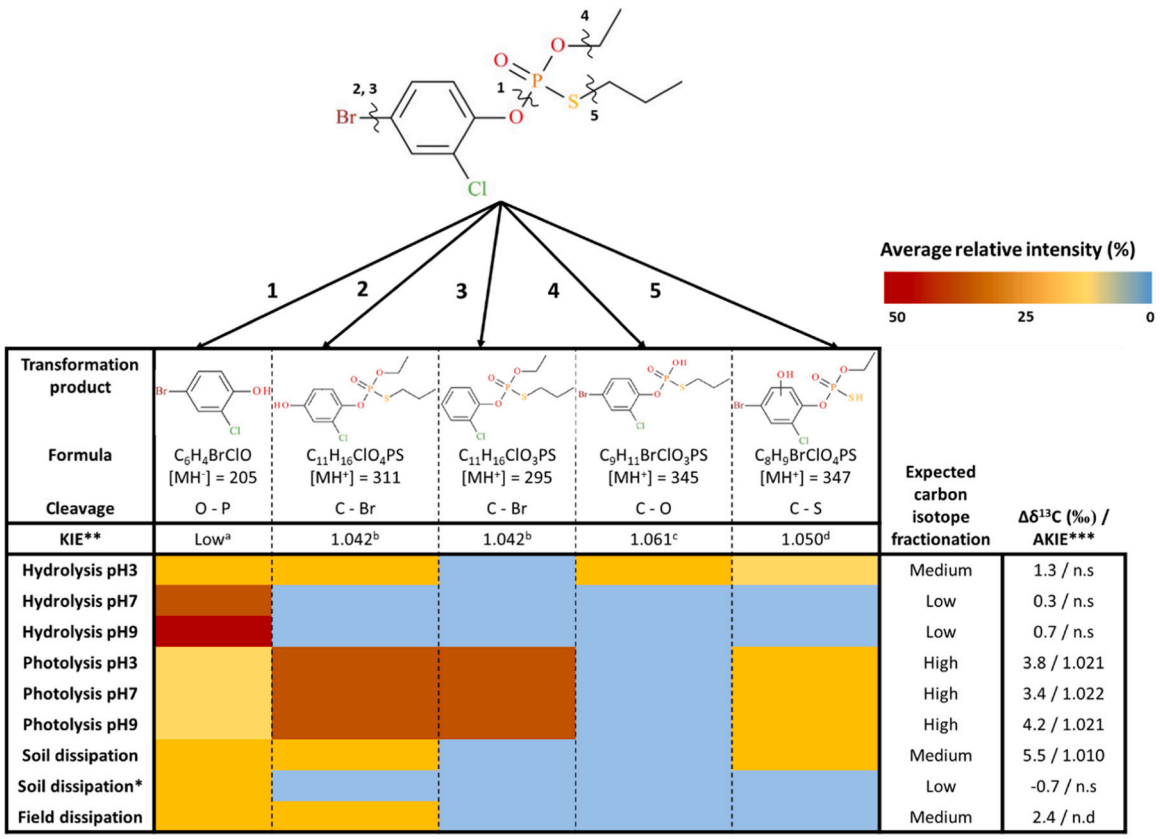

Fig. 3. Profenofos transformation products in hydrolysis, photolysis, and soil dissipation laboratory experiments. Relative intensity refers to the peak amplitude of transformation product, normalized by the intensity of the profenofos peak. Bond cleavages, formula, and [$MH^{+/-}$] masses are given in the SI and were obtained from Angthararuk et al. [50]. The occurrence of transformation products within experimental replicates varied by up to 20 %. *Heat-treated soil experiments ** Maximal expected kinetic isotope effect (KIE) determined from tabulated Streitwieser Limits *** AKIE values based on ε_c obtained in various profenofos dissipation experiments and on the most significant detected transformation products. [a] since carbon is not directly involved in the bond cleavage, the isotope effect is secondary and presumed to be minimal [51]. [b] from Palau et al. [52]. [c] from Elsner et al. [51]. [d] from Cook [53].

3.3.3. Photolysis

UV photolysis caused significant isotope fractionation, with $\Delta\delta^{13}C_{(end\ -\ initial)}$ reaching up to 4.2 ‰ at pH 9. However, stable isotope fractionation was not pH-dependent, with ε_C ranging consistently from − 1.9 to − 2.0 ‰ across the pH range of 3–9 (Table 1). Under simulated sunlight, where degradation was limited to less than 50 %, no significant isotope fractionation was detected. Four degradation products were consistently detected during the UV photolysis experiments across all pH conditions. Similar TPs were identified in the simulated sunlight experiment, though in smaller proportions due to the limited extent of dissipation (< 50 %). Structural and mass spectral similarities with previously reported findings [44,50], suggest that the two primary degradation products resulted from C—Br bond cleavage (pathways 2 and 3). Additionally, BCP (pathway 1) and another TP (pathway 5), formed through C—O bond cleavage, were detected in smaller amounts. These observations align with earlier studies, which also identified the simultaneous presence of BCP and thiophosphoric acids resulting from C—Br bond cleavage under similar UV light conditions [44,45].

The analysis of TPs and the apparent kinetic isotope effect (AKIE) values suggested the simultaneous occurrence of two degradation pathways, yielding an average AKIE of 1.021–1.022. This is consistent with isotope fractionations associated with low isotope effect (hydrolysis, KIE ~ 1.000) for O–P bond cleavage and higher isotope effects (KIE = 1.042) for C–Br bond cleavage. For comparison, the OP insecticide dimethoate exhibited $\varepsilon_C = -3.7 \pm 1.1$ ‰ (AKIE = 1.009 – 1.019) during direct photolysis, involving C—O bond cleavage [56].

3.3.4. Soil dissipation

In the biotic soil dissipation experiments, profenofos TPs were detected less frequently, with maximum detection representing only 10–20 % of the initially applied profenofos, based on HPLC-MS-MS peak area ratios (TP_{max}/$Profenofos_{initial}$). Among the detected TPs, only BCP and TP2 were observed, suggesting the concurrent occurrence of O—P and C—Br bond cleavages. Notably, BCP was also significantly detected in the heat-treated soil dissipation experiment, confirming the potential for degradation by heat-resistant microorganisms or hydrolysis on mineral surfaces [26].

Despite similar dissipation kinetics between biotic and heat-treated soils, significant carbon isotope fractionation ($\varepsilon_C = -0.9 \pm 0.4$ ‰) was observed in the biotic soil experiment, whereas no significant isotope fractionation was detected under heat-treated conditions. The observed carbon isotope fractionation in the biotic soil experiment provided further evidence of profenofos biodegradation. This is likely associated with a low isotope effect involving mainly O—P bond cleavage, though higher isotope effects linked to C—Br bond cleavage may also have partly contributed to the observed isotope fractionation. In contrast, profenofos undergoing O—P bond cleavage in the heat-treated experiments consistently showed no significant carbon isotope fractionation. By comparison, biodegradation-specific ε_C values ranging from -5.5 ± 0.1 ‰ to -7.2 ± 0.5 ‰ were previously reported during malathion degradation in slurry experiments, where metabolites indicative of C—O or C—S bond cleavage were identified [57]. However, in the biotic experiment, the multiple biodegradation pathways and the possible small mass loss of profenofos from volatilisation hindered the determination of a reaction-specific ε_C value for profenofos

biodegradation.

Overall, the combined analysis of transformation products and carbon isotopic signatures enabled (i) the determination of pathway-specific isotope fractionation as reference data (Fig. 4) and (ii) the identification and differentiation of the primary dissipation processes occurring in soil. When integrated into a specifically tailored model, this approach can be applied under complex field conditions to evaluate the environmental fate of profenofos and its TPs, as well as the associated risks on water resources.

3.4. *Profenofos dissipation in agricultural plot and transfer to groundwaters*

Profenofos concentrations in the soil of the agricultural plot were monitored during a beetroot growing season from the day before profenofos application (–1 day, dose of 240 mg.m^{-2}) up to day 34 post-application. Profenofos concentrations in the plot soil increased immediately following the application, rising from 0.1 to 375 µg.kg$^{-1}_{wet\ soil}$ (t = 0 days) (Fig. 5).

Assuming a topsoil sampling layer of 10 cm thick and a soil density of 1.4 g.cm^{-3}, the initial profenofos stock in the topsoil was estimated at 78 mg.m^{-2}, approximately three times lower than the application dose reported by the farmer. This observation aligns with previous studies, which reported only 33 % recovery of profenofos in the upper 10 cm of soil column within 3 h post-application [58]. Several factors could account for the reduced recovery rate of profenofos, including (i) uncertainties in the preparation of commercial formulation by local farmers, (ii) volatilisation from soil surfaces, and (iii) substantial drift and variability from the manual spraying practices.

Post-application, profenofos concentrations in the soil decreased to 0.5 ± 0.1 µg.kg^{-1} by 34 days. The dissipation kinetics ($T_{1/2}$ = 1.1 ± 0.6 d, assuming a first order process) were consistent with those observed in laboratory degradation experiments. Due to the rapid dissipation, $\delta^{13}C$ measurements were only feasible during the initial three sampling periods (t = 0, t = 1 and t = 3 d). As expected, the $\delta^{13}C$ value measured immediately after application (t = 0; $\delta^{13}C$ = − 23.5 ± 0.3 ‰) was not significantly different from that of the applied profenofos formulation (− 23.8 ± 0.3 ‰; ROCKET 44). Over time, isotope fractionation was observed, with $\delta^{13}C$ = − 23.2 ± 0.3 ‰ after 1 day, and $\delta^{13}C$ = − 21.0 ± 0.3 ‰ after 3 days, indicating significant in situ profenofos degradation.

Previous experiment (Fig. 4) demonstrated that both photolysis and biodegradation can result in isotopic fractionation. The $\Delta\delta^{13}C$ = 2.4 ‰ observed three days post-application suggests that either processes could be involved. However, the presence of BCP and TP2 TPs, which were associated with profenofos biodegradation, and the absence of the key photolysis degradation product TP3 (Fig. 3), strongly suggest that biodegradation was the primary dissipation processes in the field plot experiment. This conclusion aligns with results from the soil laboratory experiments, suggesting that these observations may be cautiously extrapolated to field conditions. Assuming that biodegradation was the dominant dissipation process in the soil experiment, involving bond cleavage and significant isotope fractionation, the amount of profenofos degradation in the topsoil (F, Eq. (3)) was estimated from the $\varepsilon_{Cdegradation}$ value (− 0.9 ± 0.4, Table 1) and the observed changes of $\delta^{13}C$ in the field plot. After 3 days, profenofos degradation was estimated at 96 %, consistent with the observed 95 % dissipation. This supports the conclusion that biodegradation, rather than photolysis, was the primary dissipation process, although volatilisation may have also contributed to profenofos dissipation.

To further estimate the contributions of dissipation processes of profenofos over time, a modelling approach was developed. The soil-specific model aligned well with the observed profenofos concentrations and isotope compositions in the plot (Fig. 5a). However, the discrepancy between the reported profenofos application rate (244 mg.m^{-2}) and the measured topsoil mass three hours post-application (78 mg.m^{-2}) could not be fully explained by photolysis, volatilisation, or biodegradation kinetics derived from laboratory experiments. Off-site transport via runoff or leaching was unlikely within the first two days post-application. Similar discrepancies in recovery have been attributed to drift and variability associated with manual spraying [58]. To address this, a correction factor was applied to the reported application rate, aligning the model with the initial soil measurements. The corrected model confirmed rapid profenofos dissipation in the soil, with a simulated $T_{1/2}$ of 1.3 ± 0.4 d, consistent with the observed $T_{1/2}$ of 1.1 ± 0.6 d.

By incorporating laboratory-derived ε_C values for biodegradation and photolysis, the model predicted an increase in $\delta^{13}C$ to $\Delta\delta^{13}C$ = +2.0 ‰ (ranging from + 0.8 to + 4.4 ‰; IC 95 %) by day 3, which matched the observed $\Delta\delta^{13}C$ of + 2.7 ± 0.8 ‰. A detailed analysis of model outputs allowed for the differentiation of dissipation processes, confirming that biodegradation was the dominant process, accounting for 90.5 % (from 87.0 % to 92.1 %; IC 95 %), with photolysis contributing only 7.6 % (IC 95 % < 0.2 %), and volatilisation with only 0.05 % (IC 95 % < 0.02 %) by day 7.

The model results also confirmed the low profenofos sorption in soil, with less than 0.3 % in the non-extractable fraction 34 days post-application (Fig. 5b). Additionally, the predicted low leaching potential (< 0.02 %) was consistent with the absence of profenofos (< LOD) in passive samplers (POCIS) deployed in groundwaters beneath the field

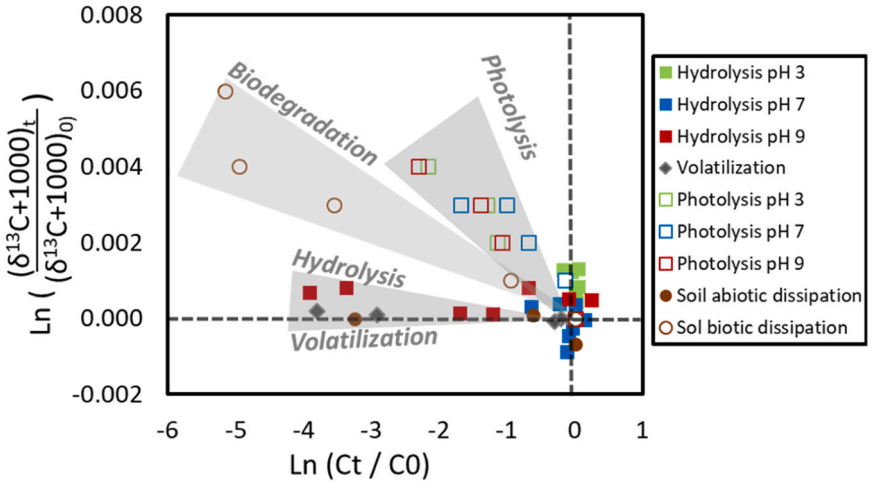

Fig. 4. Rayleigh plot derived from profenofos dissipation in hydrolysis, photolysis and soil biotic and heat-treated laboratory experiments.

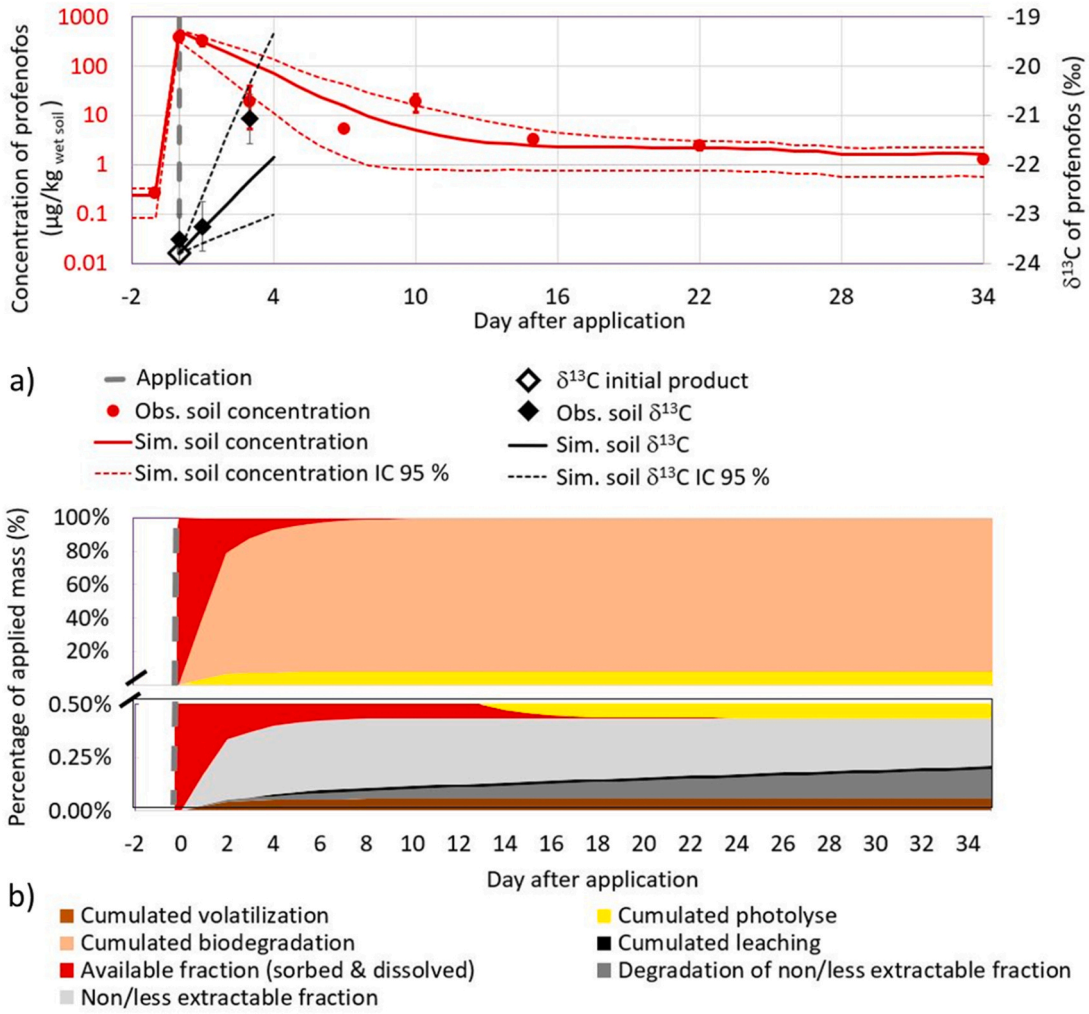

Fig. 5. a) Profenofos concentrations (red, log scale) and carbon isotope compositions ($\delta^{13}C$, black) in soil following a single application, as determined by both observational data and model simulations. Dotted red and black lines represent the 95 % confidence intervals (CI) for profenofos concentrations and carbon isotope compositions in the topsoil, respectively. b) Contribution of profenofos dissipation processes, expressed as a proportion of applied mass, as determined by the model.

plots, despite two to three crop cycles per year (e.g., sugar beets, onions or cabbages) with regular profenofos applications [31,59].

4. Conclusions

This study investigated the dissipation of profenofos in tropical agricultural soil using a GC–C–IRMS method developed for CSIA of this widely used insecticide. This method enabled the precise and accurate determination of carbon isotope ratios in profenofos, particularly for injections above 8 ng of carbon on-column, corresponding to concentrations exceeding 11 $mg.L^{-1}$ in extracts or 0.5 $\mu g.g^{-1}$ in soil. The absence of carbon isotope fractionation during water and soil extractions of profenofos ensured the applicability of this approach in both laboratory and field settings.

Abiotic dissipation experiments emphasised that profenofos undergoes rapid volatilisation from aqueous solution and photolysis under UV radiations, while hydrolysis and photolysis under simulated sunlight play minor roles under typical environmental pH and temperature conditions. Significant carbon isotope fractionation was observed during photolysis under simulated sunlight, whereas volatilisation and hydrolysis exhibited minimal or negligible isotope fractionation. Under biotic conditions, carbon isotope fractionation and the detection of transformation products indicated a significant contribution from biodegradation, which was further corroborated by modelling results in the field experiment. The study demonstrated that carbon isotope fractionation during profenofos degradation is pathway-specific rather than uniform, enabling the identification of distinct processes such as photolysis and biodegradation in field applications.

Monitoring of stable isotope signatures presents a promising method for evaluating the degradation and transformation pathways of profenofos in agroecosystems. To advance understanding of profenofos reactive transport through CSIA, additional laboratory studies are needed to establish reference isotope fractionation factors for various degradation pathways under distinct hydrogeochemical conditions. Future experiments should aim to more accurately represent field conditions, and include abiotic control experiments under more effective sterilization conditions. Additionally, integrating stable isotopes such as ^{2}H, ^{18}O, and ^{15}N in future studies could provide a more comprehensive multi-element isotope analysis framework for studying profenofos and other organophosphate pesticides in the environment.

Environmental Implication

This study highlights the dissipation of profenofos in tropical agricultural soils, with biodegradation accounting for over 90 % of its removal within three days and minimal leaching potential. By applying compound-specific isotope analysis (CSIA) of profenofos and transformation product analysis, pathway-specific carbon isotope

fractionation was identified, distinguishing photolysis from biodegradation processes. These findings provide critical insights for assessing pesticide degradation in agroecosystems, enhancing contamination risk evaluations, and guiding agricultural practices. The integration of kinetic modeling and isotope analysis represents a powerful tool for policymakers and water management agencies to develop more effective mitigation strategies against pesticide contamination in tropical environments.

CRediT authorship contribution statement

Payraudeau Sylvain: Writing – review & editing, Visualization, Validation, Software, Conceptualization. **Grail Camille:** Writing – review & editing, Investigation, Formal analysis, Conceptualization. **Masbou Jérémy:** Writing – original draft, Validation, Methodology, Investigation, Formal analysis, Data curation, Conceptualization. **Imfeld Gwenael:** Writing – review & editing, Validation, Supervision, Resources, Project administration, Methodology, Investigation, Conceptualization. **Riotte Jean:** Writing – review & editing, Resources, Project administration, Methodology, Investigation, Conceptualization. **Muddu Sekhar:** Writing – review & editing, Project administration, Methodology, Conceptualization. **Ruiz Laurent:** Writing – review & editing, Methodology, Investigation, Conceptualization.

Declaration of Competing Interest

The authors declare that they have no known competing financial interests or personal relationships that could have appeared to influence the work reported in this paper.

Acknowledgements

The study was funded by the IAEA CRP D15018 “Multiple Isotope Fingerprints to Identify Sources and Transport of Agro-Contaminants”, the ATCHA Project ANR-16-CE03-0006, and the Environmental Research Observatory M-TROPICS (https://mtropics.obs-mip.fr/), which is supported by the University of Toulouse, IRD and CNRS-INSU.

Appendix A. Supporting information

Supplementary data associated with this article can be found in the online version at doi:10.1016/j.jhazmat.2025.137428.

Data availability

Data will be made available on request.

References

[1] Liu, T., et al., 2019. A review on removal of organophosphorus pesticides in constructed wetland: performance, mechanism and influencing factors. Sci Total Environ 651, 2247–2268.
[2] Fenner, K., Canonica, S., Wackett, L.P., Elsner, M., 2013. Evaluating pesticide degradation in the environment: blind spots and emerging opportunities. Science 341 (6147), 752–758.
[3] Ragnarsdottir, K.V., 2000. Environmental fate and toxicology of organophosphate pesticides. J. Geol. Soc. 157 (4), 859–876.
[4] El-Saeid, M.H., Alghamdi, A.G., 2020. Identification of pesticide residues and prediction of their fate in agricultural soil. Air Pollut Sci 231 (6), 284.
[5] Höhener, P., et al., 2022. Multi-elemental compound-specific isotope analysis of pesticides for source identification and monitoring of degradation in soil: a review. Environ Chem Lett 1–16.
[6] Elsner, M., Imfeld, G., 2016. Compound-specific isotope analysis (CSIA) of micropollutants in the environment — current developments and future challenges. Curr Opin Biotechnol 41 (Suppl. C), S60–S72.
[7] Hofstetter, T.B., et al., 2024. Perspectives of compound-specific isotope analysis of organic contaminants for assessing environmental fate and managing chemical pollution. Nature Water 2 (1), 14–30.
[8] Alvarez-Zaldívar, P., Payraudeau, S., Meite, F., Masbou, J., Imfeld, G., 2018. Pesticide degradation and export losses at the catchment scale: in sights from compound-specific isotope analysis (CSIA). Water Res 139, 198–207.
[9] Masbou, J., Meite, F., Guyot, B., Imfeld, G., 2018. Enantiomer-specific stable carbon isotope analysis (ESIA) to evaluate degradation of the chiral fungicide metalaxyl in soils. J Hazard Mater 353, 99–107.
[10] Pérez-Rodríguez, P., Schmitt, A.-D., Gangloff, S., Masbou, J., Imfeld, G., 2021. Plants affect the dissipation and leaching of anilide pesticides in soil mesocosms: insights from compound-specific isotope analysis (CSIA). Agric Ecosyst Environ 308, 107257.
[11] Gallego, S., et al., 2024. Tracking atrazine degradation in soil combining 14C-mineralisation assays and compound-specific isotope analysis. Chemosphere 363, 142981.
[12] Xu, Z., Liu, W., Yang, F., 2018. A new approach to estimate bioavailability of pyrethroids in soil by compound-specific stable isotope analysis. J Hazard Mater 349, 1–9.
[13] Yun, H.Y., Kim, I.-S., Shin, K.-H., 2024. Compound-specific isotope analysis provides direct evidence for identifying the source of residual pesticides diazinon and procymidone in the soil–plant system. J. Agric. Food Chem.
[14] Masbou, J., Payraudeau, S., Guyot, B., Imfeld, G., 2023. Dimethomorph degradation in vineyards examined by isomeric and isotopic fractionation. Chemosphere 313, 137341.
[15] Wu, L., Kümmel, S., Richnow, H.H., 2017. Validation of GC–IRMS techniques for δ 13C and δ 2H CSIA of organophosphorus compounds and their potential for studying the mode of hydrolysis in the environment. Anal Bioanal Chem 409 (10), 2581–2590.
[16] Wu, L., et al., 2018. Carbon and hydrogen isotope analysis of parathion for characterizing its natural attenuation by hydrolysis at a contaminated site. Water Res 143, 146–154.
[17] Fang, L., et al., 2020. Enantioselective uptake determines degradation selectivity of chiral profenofos in cupriavidus nantongensis X1T. J Agric Food Chem 68 (24), 6493–6501.
[18] Verma, S., Chatterjee, S., 2021. Biodegradation of profenofos, an acetylcholine esterase inhibitor by a psychrotolerant strain Rahnella sp. PFF2 and degradation pathway analysis. Int Biodeterior Biodegrad 158, 105169.
[19] Bhandari, G., et al., 2019. Pesticide residues in Nepalese vegetables and potential health risks. Environ Res 172, 511–521.
[20] Ma, Y., Li, M., Wu, M., Li, Z., Liu, X., 2015. Occurrences and regional distributions of 20 antibiotics in water bodies during groundwater recharge. Sci Total Environ 518, 498–506.
[21] Wanwimolruk, S., Kanchanamayoon, O., Phopin, K., Prachayasittikul, V., 2015. Food safety in Thailand 2: pesticide residues found in Chinese kale (Brassica oleracea), a commonly consumed vegetable in Asian countries. Sci Total Environ 532, 447–455.
[22] Liu, X., et al., 2019. Photocatalytic degradation of profenofos and triazophos residues in the Chinese cabbage, brassica chinensis, using Ce-doped TiO2. Catalysts 9 (3), 294.
[23] Kumar, V., Sharma, N., Vangnai, A., 2021. Modeling degradation kinetics of profenofos using Acinetobacter sp. 33F. Environ Technol Innov 21, 101367.
[24] Drouin, G., et al., 2021. Direct and indirect photodegradation of atrazine and S-metolachlor in agriculturally impacted surface water and associated C and N isotope fractionation. Environ Sci: Process Impacts 23 (11), 1791–1802.
[25] LIght V, Region U. Sunlight, Weathering & Light Stability Testing.
[26] Irie, M., 2008. PROFENOFOS (171). FAO report, evaluation 08. Japan Ministry of Agriculture, Forestry and Fisheries.
[27] Baker KF. The UC system for producing healthy container-grown plants; 1957.
[28] Sekhar, M., Riotte, J., Ruiz, L., Jouquet, P., Braun, J.-J., 2016. Influences of climate and agriculture on water and biogeochemical cycles: Kabini critical zone observatory. Proc Indian Natl Sci Acad 833–846.
[29] Riotte, J., et al., 2021. The Multiscale TROPIcal CatchmentS critical zone observatory M-TROPICS dataset III: hydro-geochemical monitoring of the Mule Hole catchment, south India. Hydrol Process 35 (5), e14196.
[30] Gaillardet J, OZCAR: the French network of critical zone observatories. Vol. 17(no. 1); 2018. p. 1–24.
[31] Baccar, M., et al., 2023. Dynamics of crop category choices reveal strategies and tactics used by smallholder farmers in India to cope with unreliable water availability. Agric. Syst. 211, 103744.
[32] Gilevska T, Masbou J, Baumlin B, Imfeld G. Passive samples (POCIS) in ponds and wetlands to evaluate pesticide degradation using compound-specific isotope analysis; 2020.
[33] Gilevska, T., et al., 2022. Simple extraction methods for pesticide compound-specific isotope analysis from environmental samples. MethodsX, 101880.
[34] Gilevska, T., et al., 2022. Do pesticides degrade in surface water receiving runoff from agricultural catchments? Combining passive samplers (POCIS) and compound-specific isotope analysis. Sci Total Environ, 156735.
[35] Masbou, J., Drouin, G., Payraudeau, S., Imfeld, G., 2018. Carbon and nitrogen stable isotope fractionation during abiotic hydrolysis of pesticides. Chemosphere 213, 368–376.
[36] Coplen, T.B., 2011. Guidelines and recommended terms for expression of stable-isotope-ratio and gas-ratio measurement results. Rapid Commun Mass Spectrom 25 (17), 2538–2560.
[37] Scott, K., Lu, X., Cavanaugh, C., Liu, J., 2004. Optimal methods for estimating kinetic isotope effects from different forms of the Rayleigh distillation equation. Geochim et Cosmochim Acta 68 (3), 433–442.
[38] Payraudeau, S., Alvarez-Zaldivar, P., van Dijk, P., Imfeld, G., 2024. Constraining pesticide degradation in conceptual distributed catchment models with compound-specific isotope analysis (CSIA). EGUsphere, pp. 1–28.
[39] Allen RG, Bastiaanssen W, Tasumi M, Morse A. Evapotranspiration on the watershed scale using the SEBAL model and Landsat images. In: Proceedings of the

2001 ASAE annual meeting. American Society of Agricultural and Biological Engineers; 1998. pp. 1.
[40] Raes, D., De Nys, E., Deproost, P., 2002. UPLOW, a model to assess water and salt movement from a shallow water table to the topsoil, Atelier du PCSI (Programme Commun Systèmes Irrigués) sur une Maîtrise des Impacts Environnementaux de l'Irrigation. Cirad-IRD-Cemagref 9.
[41] Masbou, J., Höhener, P., Payraudeau, S., Martin-Laurent, F., Imfeld, G., 2024. Stable isotope composition of pesticides in commercial formulations: the ISOTOPEST database. Chemosphere, 141488.
[42] Mackay, D., Shiu, W.-Y., Lee, S.C., 2006. Handbook of physical-chemical properties and environmental fate for organic chemicals. CRC press.
[43] Siripattanakul-Ratpukdi, S., Vangnai, A.S., Sangthean, P., Singkibut, S., 2015. Profenofos insecticide degradation by novel microbial consortium and isolates enriched from contaminated chili farm soil. Environ Sci Pollut Res 22, 320–328.
[44] Zamy, C., Mazellier, P., Legube, B., 2004. Phototransformation of selected organophosphorus pesticides in dilute aqueous solutions. Water Res 38 (9), 2305–2314.
[45] Ratpukdi, T., et al., 2022. Photodegradation of profenofos in aqueous solution by vacuum ultraviolet. J Photochem Photobiol A: Chem 433, 114179.
[46] Wei, J., Furrer, G., Kaufmann, S., Schulin, R., 2001. Influence of clay minerals on the hydrolysis of carbamate pesticides. Environ Sci Technol 35 (11), 2226–2232.
[47] Palanimanickam, A., Sepperumal, U., 2018. Degradation of profenofos in soil inoculated with Bacillus cereus and Aneurinibacillus migulanus. Indian J Appl Microbiol 21 (3), 35–42.
[48] Gupta, S., Gajbhiye, V.T., Sharma, R.K., Gupta, R.K., 2011. Dissipation of cypermethrin, chlorpyriphos, and profenofos in tomato fruits and soil following application of pre-mix formulations. Environ Monit Assess 174, 337–345.
[49] Malghani, S., Chatterjee, N., Yu, H.X., Luo, Z., 2009. Isolation and identification of profenofos degrading bacteria. Braz J Microbiol 40, 893–900.
[50] Angthararuk, D., et al., 2017. Degradation products of profenofos as identified by high-field FTICR mass spectrometry: isotopic fine structure approach. J Environ Sci Health Part B 52 (1), 10–22.
[51] Elsner, M., Zwank, L., Hunkeler, D., Schwarzenbach, R.P., 2005. A new concept linking observable stable isotope fractionation to transformation pathways of organic pollutants. Environ Sci Technol 39 (18), 6896–6916.
[52] Palau, J., et al., 2023. Dual C–Br isotope fractionation indicates distinct reductive dehalogenation mechanisms of 1, 2-dibromoethane in Dehalococcoides-and Dehalogenimonas-containing cultures. Environ Sci Technol 57 (5), 1949–1958.
[53] Cook, P.F., 1991. Enzyme mechanism from isotope effects. Crc Press.
[54] Kuder, T., Philp, P., Allen, J., 2009. Effects of volatilization on carbon and hydrogen isotope ratios of MTBE. Environ Sci Technol 43 (6), 1763–1768.
[55] Torrentó, C., et al., 2021. Triple-element compound-specific stable isotope analysis (3D-CSIA): added value of Cl isotope ratios to assess herbicide degradation. Environ Sci Technol 55 (20), 13891–13901.
[56] Wu, L., Yao, J., Trebse, P., Zhang, N., Richnow, H.H., 2014. Compound specific isotope analysis of organophosphorus pesticides. Chemosphere 111, 458–463.
[57] Lian, S., Wu, L., Nikolausz, M., Lechtenfeld, O.J., Richnow, H.H., 2019. 2H and 13C isotope fractionation analysis of organophosphorus compounds for characterizing transformation reactions in biogas slurry: Potential for anaerobic treatment of contaminated biomass. Water Res 163, 114882.
[58] Tejada, A., et al., 2001. Impact of continued use of profenofos on soil as a consequence of cotton crop protection.
[59] Robert, M., et al., 2018. A dynamic model for water management at the farm level integrating strategic, tactical and operational decisions. Environ Model Softw 100, 123–135.